SLAC-PUB-3039
January 1983
(M)

PRIMARY AND LEAKAGE RADIATION CALCULATIONS AT 6, 10 AND 25 MeV*

W. R. NELSON
Stanford Linear Accelerator Center
Stanford University, Stanford, California 94305

and

P. D. LARIVIERE
Varian Associates, Inc.
Palo Alto, California 94303

ABSTRACT

Primary and leakage x-ray spectra for typical clinical accelerators have been calculated using the EGS Monte Carlo code for three energies (6, 10, 25 MeV) and four angles (0^o, 45^o, 90^o, 135^o). Broad beam transmission curves have been calculated for ordinary concrete using the MORSE program with the EGS spectra as input. A simple analytic model, which is shown to agree rather well with both experimental data and with the MORSE results, is presented and initial and subsequent tenth-value layers are extracted. Finally, the photon spectrum after the concrete shield is obtained with MORSE.

Submitted to Health Physics

---

* Work supported by the Department of Energy, contract DE-AC03-76SF00515.

INTRODUCTION

Design guidelines for the shielding of medical x-ray accelerators are well documented in the reports issued by the National Council on Radiation Protection and Measurements (NCRP70; NCRP76; NCRP77). However, as clearly pointed out by Tochilin and LaRiviere (To79), there is virtually no information on the transmission of high energy x rays emitted at angles other than zero degrees. The conventional method for shielding these facilities has been to use the tenth-value layer for the primary beam, as given in the NCRP reports, in order to determine the shield requirements for the other directions. Although this is certainly a conservative approach to the problem, and one that is quite simple to do, it can result in shielding dimensions that are too large and costly, particularly in those situations where the accelerator room already exists and additional lateral shielding cannot be included easily. Certainly this was one of the motivating factors for the experiment by Tochilin and LaRiviere (To79), the results of which seem to indicate that the x-ray spectrum emanating from the shielded head of the Varian Clinac 18 is indeed softer than that of the primary beam operating in the 10 MeV mode.

The purpose of this paper is to present the results of a series of calculations to determine (1) the photon spectrum into the forward angle cone from a typical target (primary x rays), (2) the spectrum emanating at large angles from a typical accelerator head shield (leakage x rays), (3) the attenuation properties of both of these components in ordinary concrete ($\rho = 2.35\ g/cm^3$), and (4) the resultant photon spectrum on the downstream side of the shielding. The scattered radiation component, however, will not be the subject of this study.

Both the primary and leakage spectra were obtained with the EGS Monte Carlo code (Fo78) and the results were used as input to the combinatorial geometry version of MORSE (St76), as well as input for a rather simple analytic model for transmission

based on the product of attenuation and buildup integrated over all energies. The results are compared with data published in the NCRP reports and with the experimental data obtained by Tochilin and LaRiviere (To79) at 10 MeV. The selection of the energies, angles, targets, shields, and dimensions that were used in these calculations are typical of clinical accelerators currently in use. Another experimental study at 24 MeV has recently been performed by LaRiviere in order to further check the validity of these calculations, and the paper following this one contains that work.

THE EGS CODE AND X-RAY CALCULATIONS

The EGS Code System is a package of computer programs that was originally written in order to simulate the development of high energy electromagnetic cascade showers in various media by the Monte Carlo method (Fo78). More recently, however, EGS has been used to solve a variety of low energy electron-photon transport problems as well (Ne80, In82, Ro82a). The kinetic energy range for which EGS was designed extends from 100 GeV down to 100 keV for photons and 1 MeV for electrons and positrons, although recent studies have taken photons down as low 1 keV and charged particles down to 10 keV (Pe82, Ro82b). Written in an extended FORTRAN language called MORTRAN (Co75), EGS is extremely versatile in that electron-photon transport can be performed in any element, compound, or mixture of these elements. The major processes that are accounted for in the transport are: bremsstrahlung, discrete Bhabha and Moller scattering, excitation and ionization (including density effect), annihilation at rest and in flight, multiple Coulomb scattering (according to Moliere), photoelectric effect, Compton scattering, and pair production. The geometry and scoring are left up to the ingenuity of the user and very sophisticated EGS User Codes have been written that take advantage of the efficiency and versatility of the system.

EGS was used in a rather simple and straight forward way in this study in order to determine the photon energy spectrum that is produced at various angles from a target struck by an incident electron beam of energies 6, 10, and 25 MeV. Two target geometries were studied. The primary radiation target (Fig. 1) consisted of semi-infinite slabs, representing the target plus the beam flattener, with material composition being different for each machine energy as given in Table 1. The electron beam entered normal to the slab surface and the photons were sorted into energy bins as they emanated from the downstream slab into a polar angle of $0^o - 15^o$, irrespective of azimuth.

The leakage radiation geometry was even simpler, as shown in Fig. 2. The EGS calculation was initiated with an electron beam at the center of a homogeneous, six inch diameter tungsten sphere, representing the production target as well as the accelerator head shielding. The photon energy spectrum was obtained for three polar angle intervals: 45^o $(35^o - 55^o)$, 90^o $(80^o - 100^o)$, and 135^o $(125^o - 145^o)$.

Electrons and positrons were followed until they fell below a cutoff energy of 1.0 MeV and photons were followed down to 100 keV. At these energies the remaining energy of the particles was deposited at that point. The results are plotted in Figs. 3(a) through 3(c) for the primary beam geometry, and in Figs. 4 through 6 for the leakage radiation situation. The narrow peak near 0.5 MeV in all the figures is due to positron annihilation. The average energy that is shown on each plot was determined from the equation

$$k_{ave} = \frac{\int_{k_{min}}^{E_0} kS(k)\,dk}{\int_{k_{min}}^{E_0} S(k)\,dk} \tag{1}$$

where E_0 is the incident kinetic energy of the electron (MeV), k_{min} is the photon cutoff energy (MeV), and S is the differential photon energy spectrum ($MeV^{-1}\ sr^{-1}$) per incident electron. A complete tabulation of the average energy of the primary and leakage radiation is given in Tables 2 and 3, respectively. It should be noted that the

average energy is quite insensitive to k_{min} values less than 100 keV, which supports our choice of the photon cutoff energy.

TRANSMISSION CALCULATIONS – A SIMPLE ANALYTIC MODEL

A simple model for the transmission of photons through a shield can be written in terms of an integral over the photon energy spectrum, S $(MeV^{-1}\ sr^{-1})$ per incident electron. That is, the absorbed dose at any given shield thickness, x (cm), is given by

$$D(x) = \frac{1.6 \times 10^{-8}}{R^2} \int_{k_{min}}^{E_0} kS(k)\ \frac{\mu_{en}(k)}{\rho_{air}}\ B(k, \mu x)\ e^{-\mu(k)x}\ dk \qquad (2)$$

where μ (cm^{-1}) is the linear attenuation coefficient of the shield, B is the absorbed dose buildup factor, μ_{en}/ρ_{air} $(cm^2\ g^{-1})$ is the mass energy absorption coefficient for air, and R (cm) is the distance from the source to the detector. The conversion factor (g-rad/MeV) and the $1/R^2$ factor outside the integral are not important since we are only interested in the transmission defined by the ratio, $D(x)/D(0)$. In using the energy absorption coefficient the assumption is made that charged particle equilibrium (CPE) conditions exist (Ka78). Broad beam geometry is accomplished by means of the buildup factor together with the exponential attenuation. The absorbed dose buildup factor that we use

$$B(k, \mu x) = 1 + \alpha(k)\mu x\ e^{\beta(k)\mu x} \qquad (3)$$

is generally referred to as the Berger form. The parameters, $\alpha(k)$ and $\beta(k)$, were taken from the work of Trubey (Tr66) corresponding to a point isotropic source in an infinite medium. The attenuation coefficients for concrete and the energy absorption coefficients for air are from Hubbell (Hu69). Air was chosen for the detector, but calculations using water resulted in insignificant differences in the results presented here.

A computer program (LEAKAGE) was written in order to perform the integration above and to determine the transmission using the EGS spectra given in the previous section. The code was originally applied to leakage spectra data, but the model and program can be applied to any spectrum, including the primary beam one. The results are presented in Figs. 7(a) through 7(c) for both the primary and leakage radiation geometries. The first, second, and third tenth-values layers ($TVL_1/TVL_2/TVL_3$) are given in Table 4.

As an independent check on the EGS/LEAKAGE model, broad beam transmission in concrete was calculated using the MORSE Monte Carlo code (St76) with EGS spectra as input (after rebinning into the 21-groups required by MORSE). Broad beam conditions were approximated in MORSE by choosing an isotropic point source centered 8 meters from the downstream face of a 20 m $\times$ 20 m concrete slab. The absorbed dose was determined using a point source estimator (see St76) and with a detector located one meter further downstream from the slab (i.e., at 9 meters). The location of the upstream face of the slab was allowed to vary towards the source for a maximum slab thickness of 80 cm. In order to insure that all parts of the EGS spectrum were reasonably well accounted for in the calculation, the reciprocal of the spectrum was selected as an importance function, thereby forcing all energies to be equally sampled with appropriate weighting applied to the results. However, path length stretching, splitting, Russian rouletting, and other variance reduction techniques were not used. As a result, slab thicknesses larger than 80 cm resulted in a "deep penetration" problem and the cost of running the calculation became prohibitive.

COMPARISON OF THE EGS/LEAKAGE MODEL WITH MORSE AND WITH EXPERIMENT

The MORSE results are shown in Figs. 7(a) through 7(b) for the primary beam case and for 45^o leakage radiation. Although some of the points appear to be systematically lower than the EGS/LEAKAGE results by as much as 25%, particularly in the 25 MeV case, the agreement is still reasonably good. MORSE calculations were also done at 90^o and 135^o for all three energies and the results, although not shown in the figures, are similar in comparison.

The primary beam results can be compared directly with published experimental data as summarized in Fig. 8 taken from NCRP77. It is apparent that the EGS/LEAKAGE model agrees rather well with the 6 and 10 MeV curves, and that the 25 MeV calculation is consistent with the curves between 20 MeV and 176 MeV (it should be noted that the 86 MeV label in Fig. 8 is a correction to the actual label (36 MeV) given in NCRP77).

The EGS/LEAKAGE model can also be compared with the recent experiment by Tochilin and LaRiviere (To79) at 10 MeV, as shown in Fig. 9, where excellent agreement is seen for the primary radiation case, but the leakage radiation results are systematically a factor of 2 to 3 lower than the model. The procedure used by Tochilin and LaRiviere to obtain the transmission consisted of making a meaurement of the dose transmitted through the shield and dividing the result by the unattenuated dose as obtained from a calculation. For the primary beam situation this procedure was quite reasonable since the dosimetry associated with the unattenuated therapy beam was obviously well understood. Furthermore, measurements were made with various field sizes in order to obtain a broad beam situation (the primary radiation point in Fig. 9 represents the maximum field size of $35 \times 35\ cm^2$).

The method of determining the unattenuated dose for the leakage radiation is subject to much higher uncertainty, particularly in terms of systematic error. The calculation was based on dosimetry measurements, performed at various angles around the accelerator head, relative to the primary beam dose at the isocenter. The unattenuated dose at the detector location was then obtained assuming that the leakage radiation decreased with distance as $1/R^2$. It is conceivable that the $1/R^2$ assumption is responsible for part, if not all, of the disagreement. Other possible explanations are that there are additional sources of radiation inside the accelerator and/or that the head shielding is not well represented by the 6 inch diameter tungsten sphere used in the EGS calculations (e.g., there are weak spots in the head shield). The primary beam calculations, on the other hand, are based on rather well defined target geometries. Certainly it calls for additional experimentation in order to better understand the nature of the leakage radiation component inside the shielded room, irrespective of any extraneous sources (i.e., scattered primary beam, etc.).

SPECTRA OUTSIDE A THICK SHIELD

The incident photon spectrum will be changed as a result of interactions within the shield and this information can be obtained from MORSE, as shown in Figs. 10(a) through 10(c) for the three incident energies studied. In these figures the 90^o leakage radiation is compared with the new spectrum after 60 cm of concrete. The histograms have been normalized such that the total photon number is one. As expected, there are more low energy photons after transmission through the concrete. For the 6 and 10 MeV energies this results in a decrease in the average energy. For the 25 MeV case, however, there is also a slight increase in the number of high energy photons, so that the average energy actually increases somewhat. A possible explanation of this might be the dominance of pair production above 10 MeV.

SUMMARY AND CONCLUSIONS

The Electron-Gamma Shower program, EGS, has been used in order to obtain x-ray spectra typical of electron linacs used for radiation therapy. Both primary and leakage radiation spectra have been presented for electron energies of 6, 10, and 25 MeV, using target geometries representative of accelerators at these energies. Because shielding studies involving the use of Monte Carlo codes, such as MORSE, are time consuming and costly, a simple analytic expression for absorbed dose transmission is given. Using this model, along with the EGS spectra, transmission curves for both the primary and leakage radiation fields are presented for concrete. The same spectra are used as input to MORSE and reasonable agreement is found, especially for the primary beam case.

The primary beam results are also found to be in excellent agreement at all three energies with experimental data recommended by the National Council on Radiation Protection and Measurements (NCRP77), as well as with a recent measurement at 10 MeV by Tochilin and LaRiviere (To79). However, the leakage radiation data by Tochilin and LaRiviere are a factor of 2 to 3 lower than the results presented here, suggesting that additional experiments should be performed in order to resolve the discrepancy. On the other hand, the basic idea of Tochilin and LaRiviere, that the leakage component is softer and easier to shield than the primary, is born out by the present calculations.

ACKNOWLEDGEMENTS

We thank Dr. Richard McCall of the SLAC Radiation Physics Group for very helpful discussions and for general support of this search.

REFERENCES

Co75 Cook A. J. and Shustek L. J., 1975, A User's Guide to MORTRAN2, Stanford Linear Accelerator Center, 2575 Sand Hill Road, Menlo Park, CA 94025, Computation Research Group Report No. CGTM-165.

Fo78 Ford R. L. and Nelson W. R., 1978, The EGS Code System : Computer Programs for the Monte Carlo Simulation of Electromagnetic Cascade Showers (Version 3), Stanford Linear Accelerator Center, 2575 Sand Hill Road, Menlo Park, CA 94025, Report No. SLAC-210,

Hu69 Hubbell J. H., 1969, Photon Cross Sections, Attenuation Coefficients, and Energy Absorption Coefficients from 10 keV to 100 GeV, National Bureau of Standards, Center for Radiation Research, Radiation Theory Section, Washington, DC 20234, Report No. NSRDS-NBS-29.

Ka68 Karzmark C. J. and Capone T., 1968, "Measurements of 6 MV X-Rays: 1. Primary Radiation Absorption in Lead, Steel, and Concrete," Br. J. Radiol. 41, 33.

Ka78 Kase K. R. and Nelson W. R., 1978, Concepts of Radiation Dosimetry, p.139ff (New York: Pergamon Press).

Ki54 Kirn F. S. and Kennedy R. J., 1954, "How Much Concrete for Shielding: Betatron X-Rays," Nucleonics 12 (6), 44.

In82 Ing H., Nelson W. R. and Shore R. A., 1982, "Unwanted Photon and Neutron Radiation Resulting from Collimated Photon Beams Interacting with the Body of Radiotherapy Patients," Medical Phys. 9, 27.

Mi56 Miller C. W. and Kennedy R. J., 1956, "Attenuation of 86 and 176 MeV Synchrotron X-Rays in Concrete and Lead," Radiat. Res. 4, 360.

NCRP70 National Council on Radiation Protection and Measurements, 1970, Medical X-Ray and Gamma-Ray Protection for Energies up to 10 MeV, 7910 Woodmont Avenue, Washington DC 20014, NCRP Report No. 34.

NCRP76 National Council on Radiation Protection and Measurements, 1976, Structural Shielding Design and Evaluation for Medical Use of X-Rays and Gamma-Rays of Energies up to 10 MeV, 7910 Woodmont Avenue, Washington, DC 20014, NCRP Report No. 49.

NCRP77 National Council on Radiation Protection and Measurements, 1977, Radiation Protection Guidelines for 0.1-100 MeV Particle Accelerator Facilities, 7910 Woodmont Avenue, Washington DC 20014, NCRP Report No. 51.

Ne80 Nelson W. R. and Jenkins T. M. (Editors), 1980, Computer Techniques in Radiation Transport and Dosimetry (New York: Plenum Press).

Pe82 Perez-Mendez V., Del Guerra A., Nelson W. R. and Tam K. C., 1982, The Imaging Performance of a Multiwire Proportional Chamber Positron Camera, Lawrence Berkeley Laboratory Report No. LBL-14114; in Proc. Int. Symp. Med. Imaging and Image Interpretation, Berlin, W. Germany, October, 1982, p.99.

Ro82a Rogers D. W. O., 1982, "More Realistic Monte Carlo Calculations of Photon Detector Response Functions," Nucl. Instrum. Methods 199, 531.

Ro82b Rogers D. W. O., 1982, "Fluence to Dose Equivalent Conversion Factors Calculated with EGS3 for Electrons from 100 keV to 20 GeV and Photons from 20 keV to 20 GeV;" Submitted to Health Physics.

St76 Straker E. A., Stevens P. N., Irving D. C. and Cain V. R., 1976, General Purpose Monte Carlo Multigroup Neutron and Gamma-Ray Transport Code with Combinatorial Geometry, Oak Ridge National Laboratory, P. O. Box X, Oak Ridge, TN 37830, RSIC Computer Code Collection, CC-203.

To79 Tochilin E. and LaRiviere P. D., 1979, "Attenuation of Primary and Leakage Radiation in Concrete for X-Rays from a 10 MV Linear Accelerator," Health Phys. 36, 387.

Tr66 Trubey D. K., 1966, A Survey of Empirical Functions Used to Fit Gamma-Ray Buildup Factors, Oak Ridge National Laboratory, P. O. Box X, Oak Ridge, TN 37830, Report No. ORNL-RSIC-10.

Table 1

Primary Radiation Target Composition
(including beam flattener)

	Slab Thickness (cm)			
Electron Kinetic Energy	Slab#1	Slab#2	Slab#3	Slab#4
6 MeV	0.10 W	0.15 Cu	1.44 Pb	--
10 MeV	0.50 Cu	1.93 W	0.47 Al	--
25 MeV	0.08 W	0.72 Cu	1.00 Al	7.62 Fe

Table 2

Average Photon Energy (MeV) of Primary Radiation for Various Incident Electron Energies

	Electron Kinetic Energy		
Angle (degrees)	6 MeV	10 MeV	25 MeV
0 – 15	1.76	2.55	4.75

Table 3

Average Photon Energy (MeV) of Leakage Radiation
at Various Angles and Incident Electron Energies

	Electron Kinetic Energy		
Angle (degrees)	6 MeV	10 MeV	25 MeV
15 – 35	1.82	2.10	2.39
35 – 55	1.63	1.77	1.91
55 – 80	1.50	1.65	1.68
80 – 100	1.43	1.51	1.59
100 – 125	1.38	1.51	1.54
125 – 145	1.34	1.47	1.59
145 – 160	1.43	1.38	1.59
160 – 180	1.42	1.52	1.57

Table 4

First, Second, and Third Tenth-Value Layers
($TVL_1/TVL_2/TVL_3$) for Ordinary Concrete ($\rho = 2.35g\ cm^{-3}$)

	Electron Kinetic Energy		
Angle (degrees)	6 MeV	10 MeV	25 MeV
Primary (0 – 15)	36.7/31.3/32.3 cm 14.4/12.3/12.7 in	41.0/36.6/37.7 cm 16.1/14.4/14.8 in	48.2/45.4/45.6 cm 19.0/17.9/18.0 in
Leakage (35 – 55)	35.3/28.6/29.3 cm 13.9/11.3/11.5 in	36.6/31.1/32.8 cm 14.4/12.2/12.9 in	37.7/33.8/36.7 cm 14.8/13.3/14.4 in
Leakage (80 – 100)	34.1/27.5/28.4 cm 13.4/10.8/11.2 in	34.9/29.3/31.1 cm 13.7/11.5/12.2 in	35.9/31.9/34.7 cm 14.1/12.6/13.7 in
Leakage (125 – 145)	33.3/26.1/26.9 cm 13.1/10.3/10.6 in	34.7/28.6/29.9 cm 13.7/11.3/11.8 in	35.5/30.5/32.5 cm 14.0/12.0/12.8 in

FIGURE CAPTIONS

Fig. 1. Semi-infinite, multi-slab target geometry used in EGS for primary radiation calculations.

Fig. 2. Tungsten sphere (6 inch diameter) target geometry used in EGS for leakage radiation calculations.

Figs. 3(a)-(c). Primary x-ray beam spectra obtained with EGS at 6, 10, and 25 MeV, respectively.

Figs. 4-6. Leakage x-ray spectra obtained with EGS at 6, 10, and 25 MeV, and for angular bins centered around 45^o, 90^o, and 135^o.

Figs. 7(a)-(c). Broad beam transmission curves in ordinary concrete ($\rho = 2.35\ g/cm^3$) for both primary and leakage components produced by electron beams of 6, 10, and 25 MeV, respectively. The curves are calculated using the EGS/LEAKAGE computer codes. The data points are MORSE results for the primary beam case and for leakage radiation (at 45^o only).

Fig. 8. Comparison of the EGS/LEAKAGE transmission results with experimental data compiled by the National Council on Radiation Protection and Measurements (NCRP77). [Note: 6 MeV (Ka68); 10, 20, and 38 MeV (Ki54); 86 and 176 MeV (Mi56)].

Fig. 9. Comparison of the EGS/LEAKAGE transmission results with experimental data for both the primary and leakage radiation (45^o, 90^o, 135^o) components produced by a 10 MeV electron beam.

Figs. 10(a)-(c). Comparision of the transmitted (solid histogram) and the incident (dashed histogram) spectra after 60 cm of concrete for 90^o leakage x-rays produced by 6, 10, and 25 MeV electrons, respectively. The histograms have been normalized to a total photon number of unity.

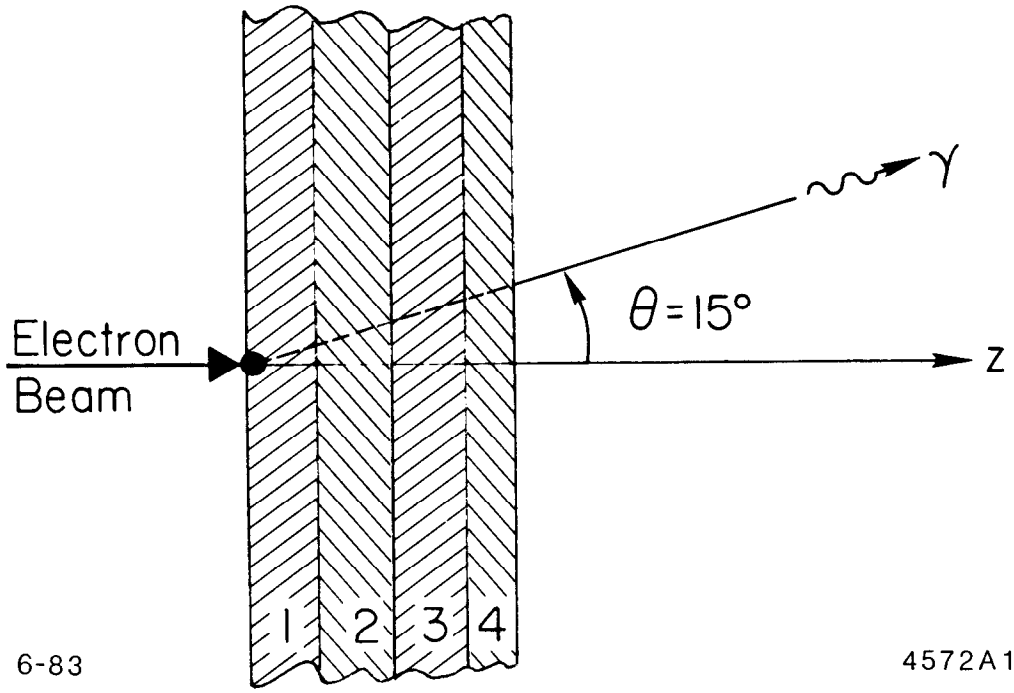

Fig. 1

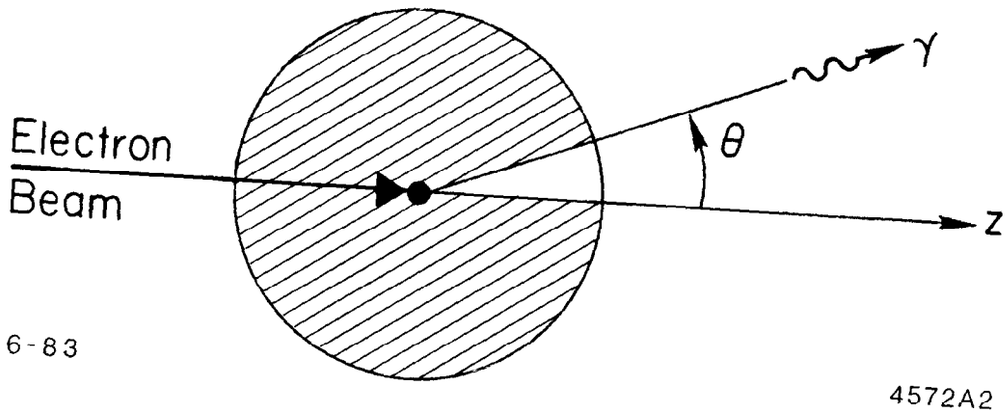

Fig. 2

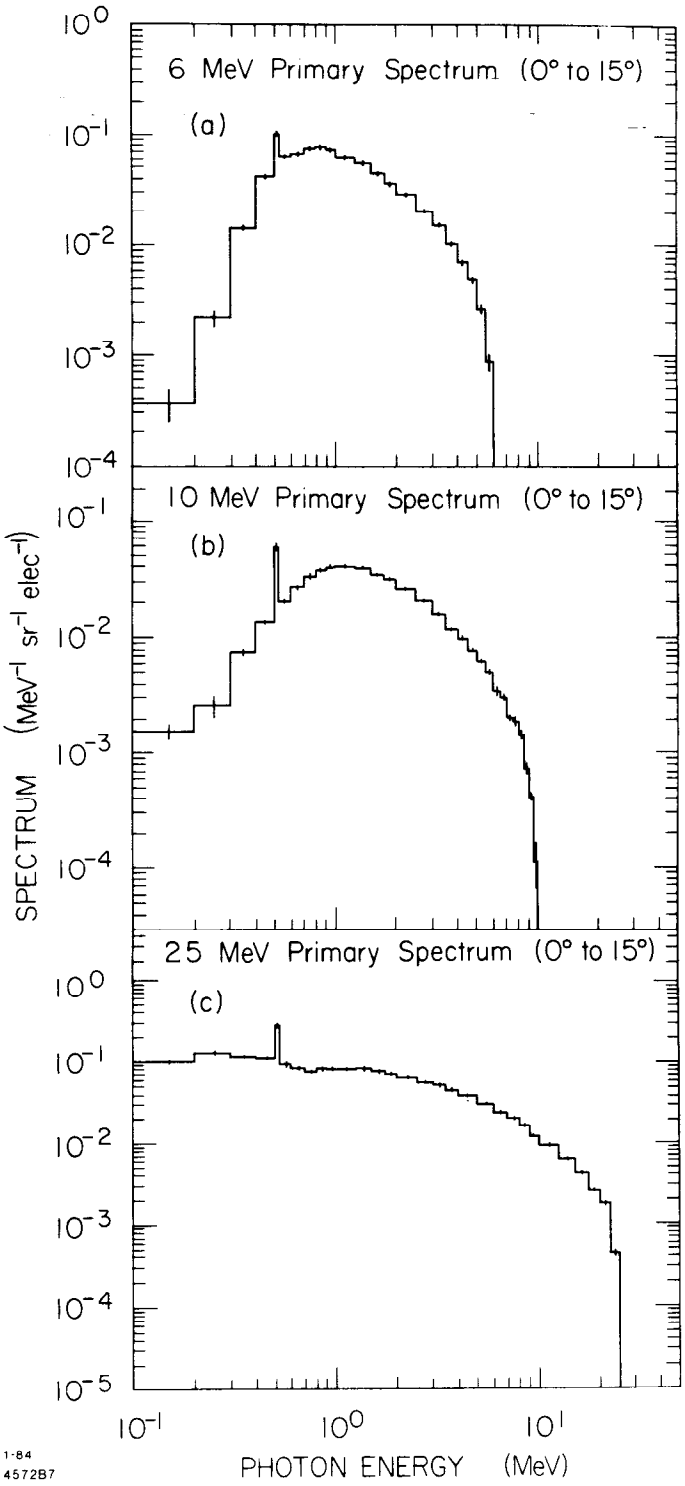
6 MeV Primary Spectrum (0° to 15°)
(a)
10 MeV Primary Spectrum (0° to 15°)
(b)
25 MeV Primary Spectrum (0° to 15°)
(c)
SPECTRUM (MeV⁻¹ sr⁻¹ elec⁻¹)
PHOTON ENERGY (MeV)
1-84
4572B7

Fig. 3

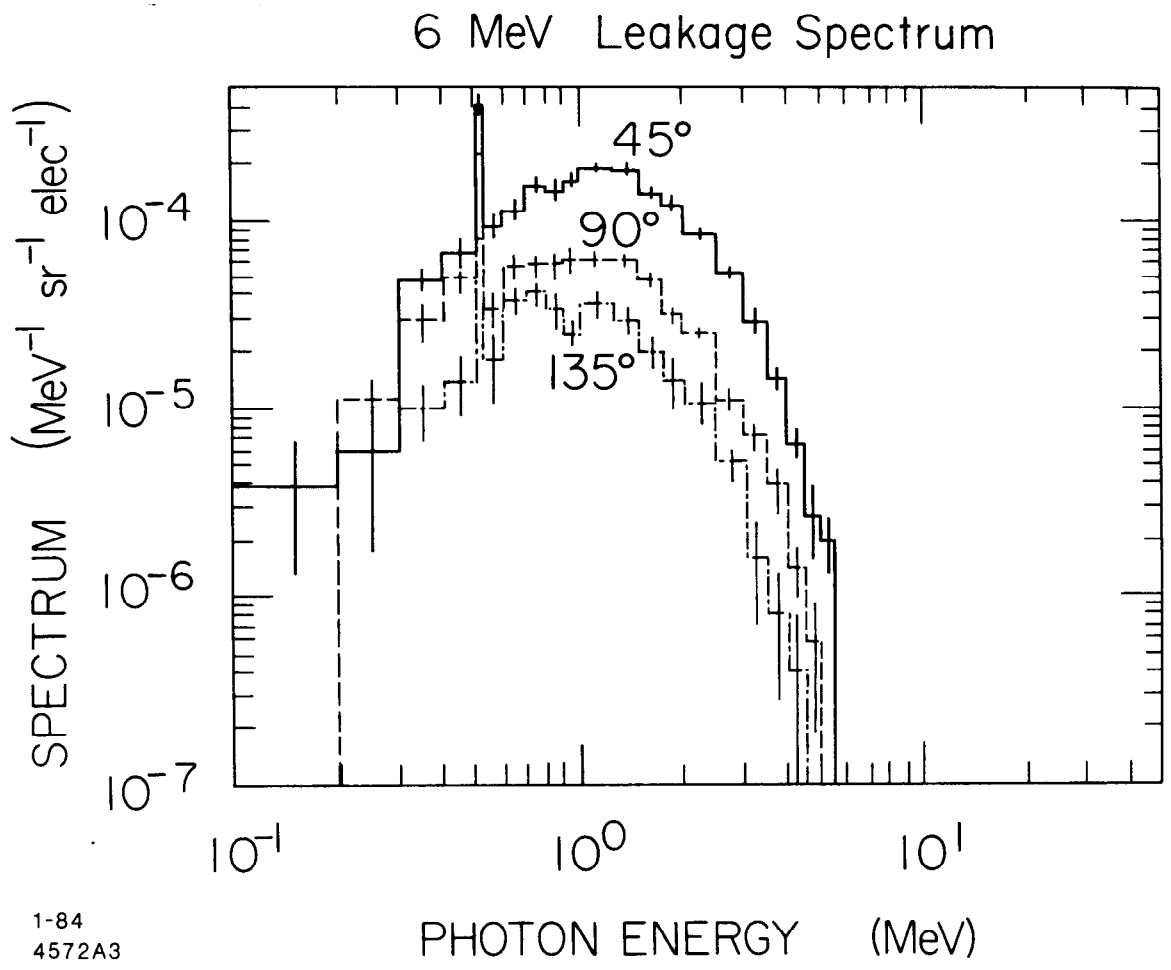
6 MeV Leakage Spectrum
45°
90°
135°
SPECTRUM (MeV⁻¹ sr⁻¹ elec⁻¹)
10⁻⁴
10⁻⁵
10⁻⁶
10⁻⁷
10⁻¹
10⁰
10¹
PHOTON ENERGY (MeV)
1-84
4572A3

Fig. 4

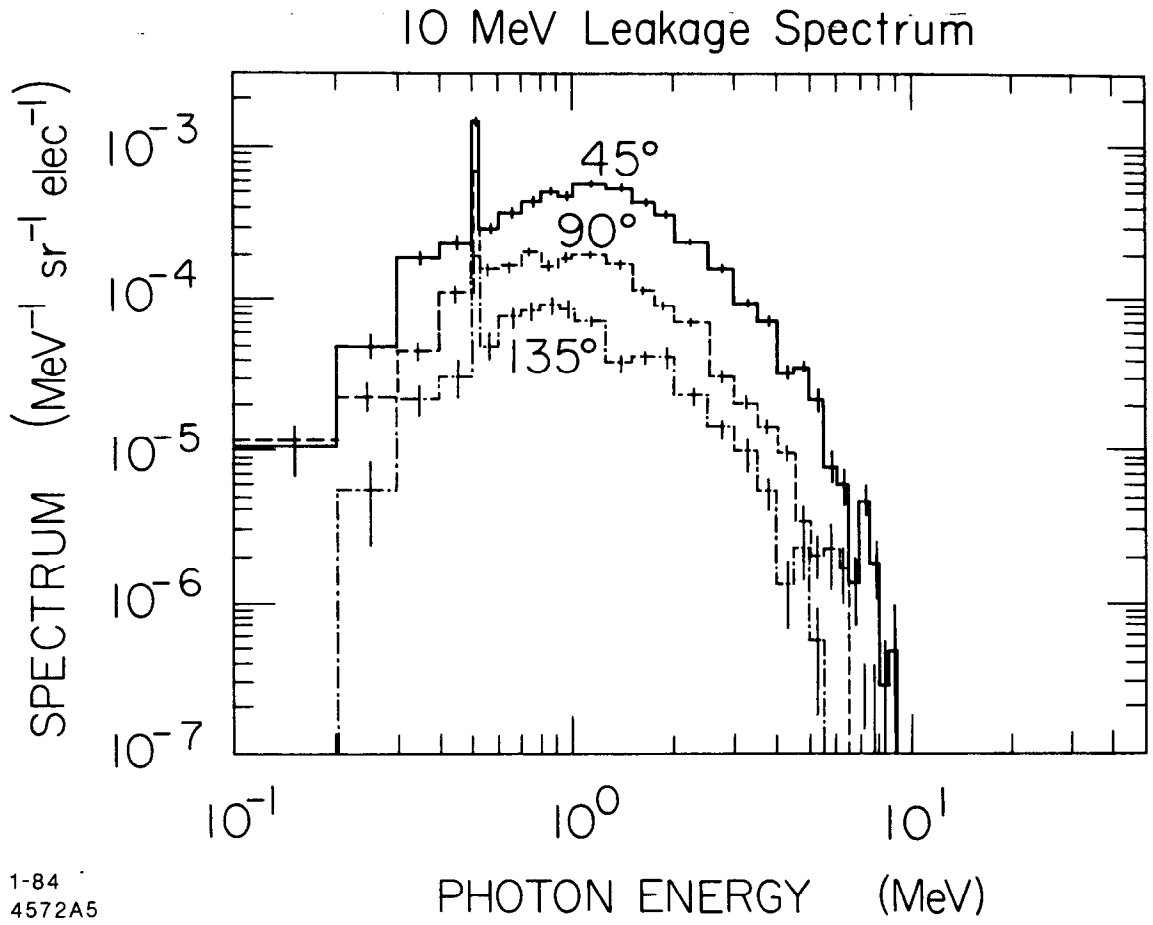
10 MeV Leakage Spectrum
SPECTRUM (MeV⁻¹ sr⁻¹ elec⁻¹)
10⁻³
10⁻⁴
10⁻⁵
10⁻⁶
10⁻⁷
45°
90°
135°
10⁻¹
10⁰
10¹
PHOTON ENERGY (MeV)
1-84
4572A5

Fig. 5

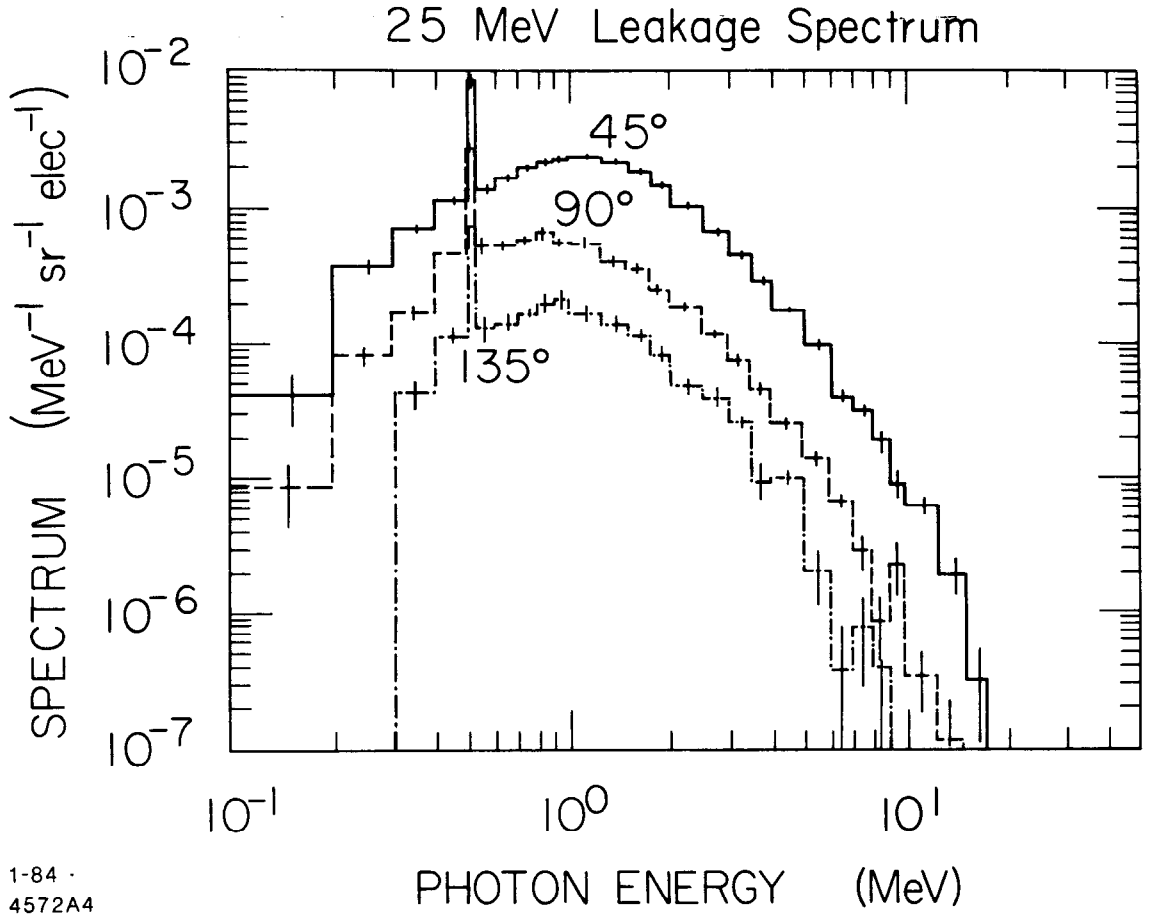
25 MeV Leakage Spectrum
SPECTRUM (MeV^{-1} sr^{-1} elec^{-1})
10^{-2}
10^{-3}
10^{-4}
10^{-5}
10^{-6}
10^{-7}
45°
90°
135°
10^{-1}
10^{0}
10^{1}
PHOTON ENERGY (MeV)
1-84
4572A4

Fig. 6

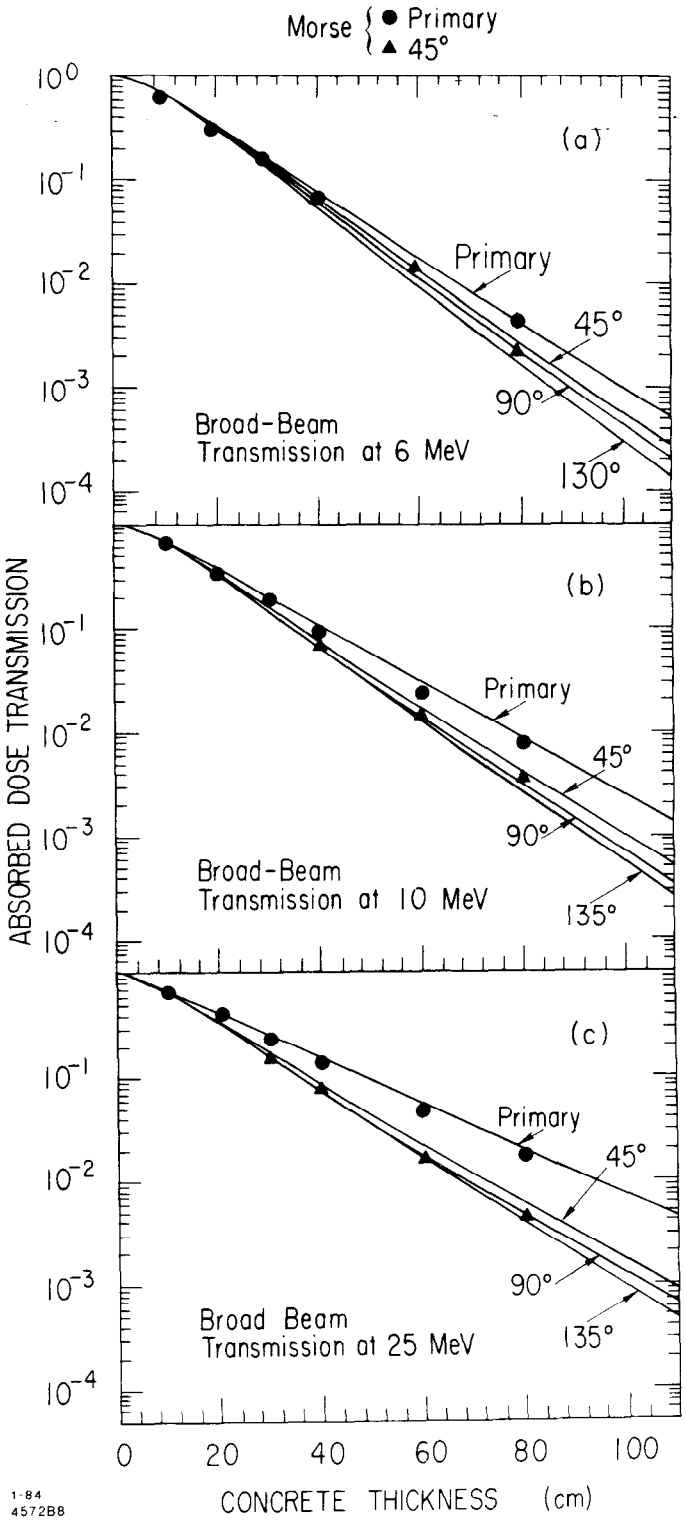
Morse { ● Primary
▲ 45°
(a)
Primary
45°
90°
130°
Broad-Beam
Transmission at 6 MeV
(b)
Primary
45°
90°
135°
Broad-Beam
Transmission at 10 MeV
(c)
Primary
45°
90°
135°
Broad Beam
Transmission at 25 MeV
ABSORBED DOSE TRANSMISSION
10^{0}
10^{-1}
10^{-2}
10^{-3}
10^{-4}
0
20
40
60
80
100
CONCRETE THICKNESS (cm)
1-84
4572B8

Fig. 7

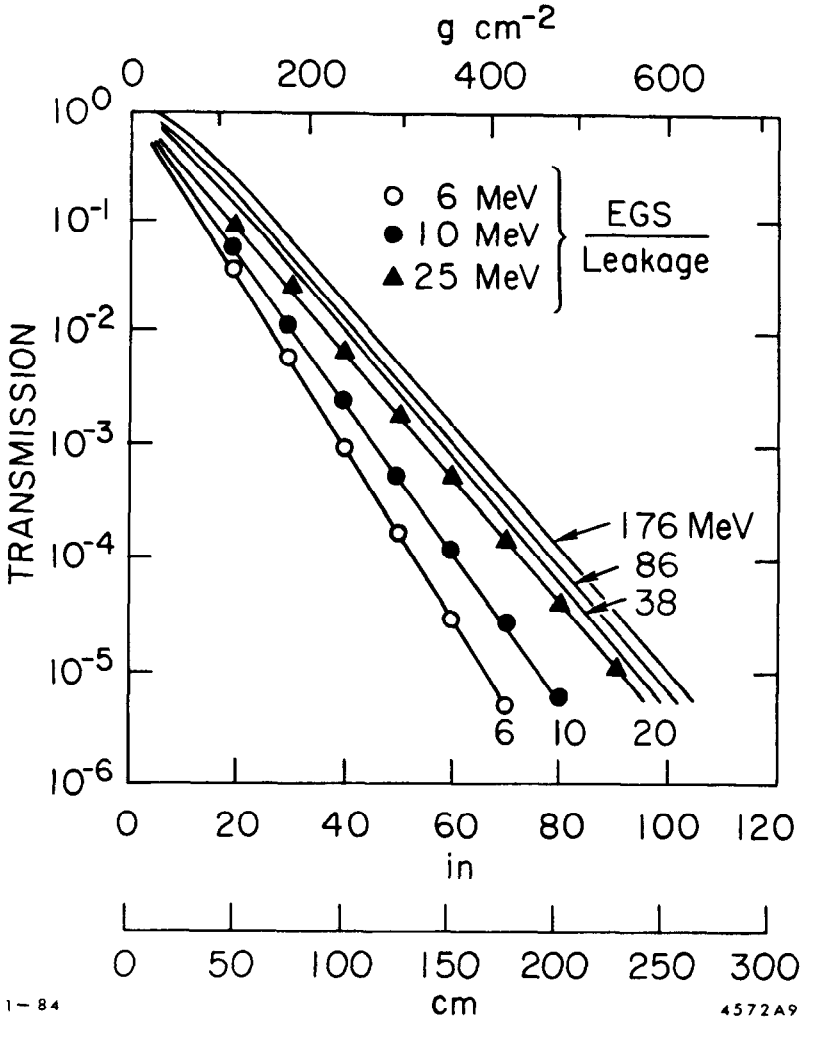
g cm^{-2}
0
200
400
600
10^0
10^{-1}
10^{-2}
10^{-3}
10^{-4}
10^{-5}
10^{-6}
TRANSMISSION
o 6 MeV
● 10 MeV
▲ 25 MeV
EGS
Leakage
176 MeV
86
38
6
10
20
0
20
40
60
80
100
120
in
0
50
100
150
200
250
300
cm
1-84
4572A9

Fig. 8

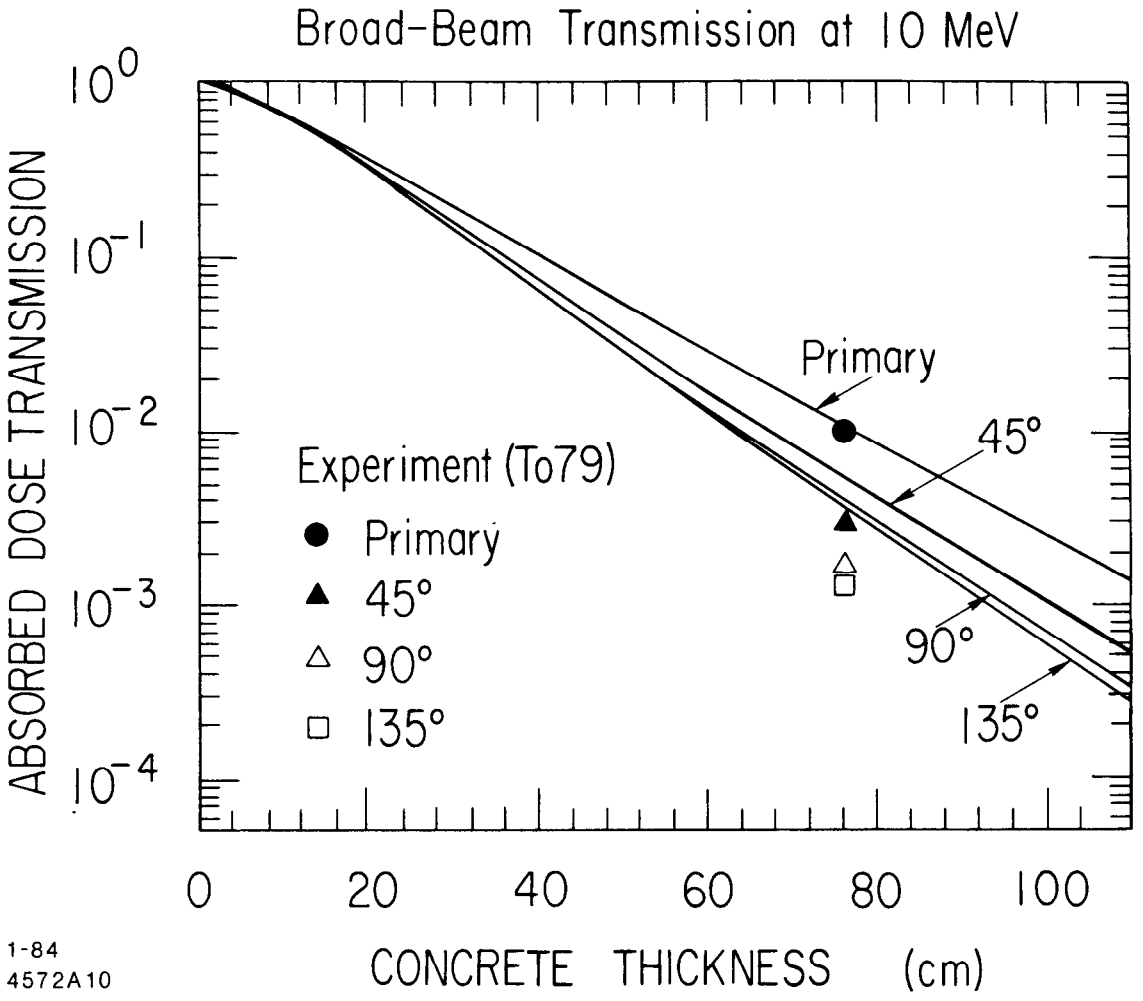
Broad-Beam Transmission at 10 MeV
ABSORBED DOSE TRANSMISSION
10^{0}
10^{-1}
10^{-2}
10^{-3}
10^{-4}
Primary
45°
90°
135°
Experiment (To79)
Primary
45°
90°
135°
0
20
40
60
80
100
CONCRETE THICKNESS (cm)
1-84
4572A10

Fig. 9

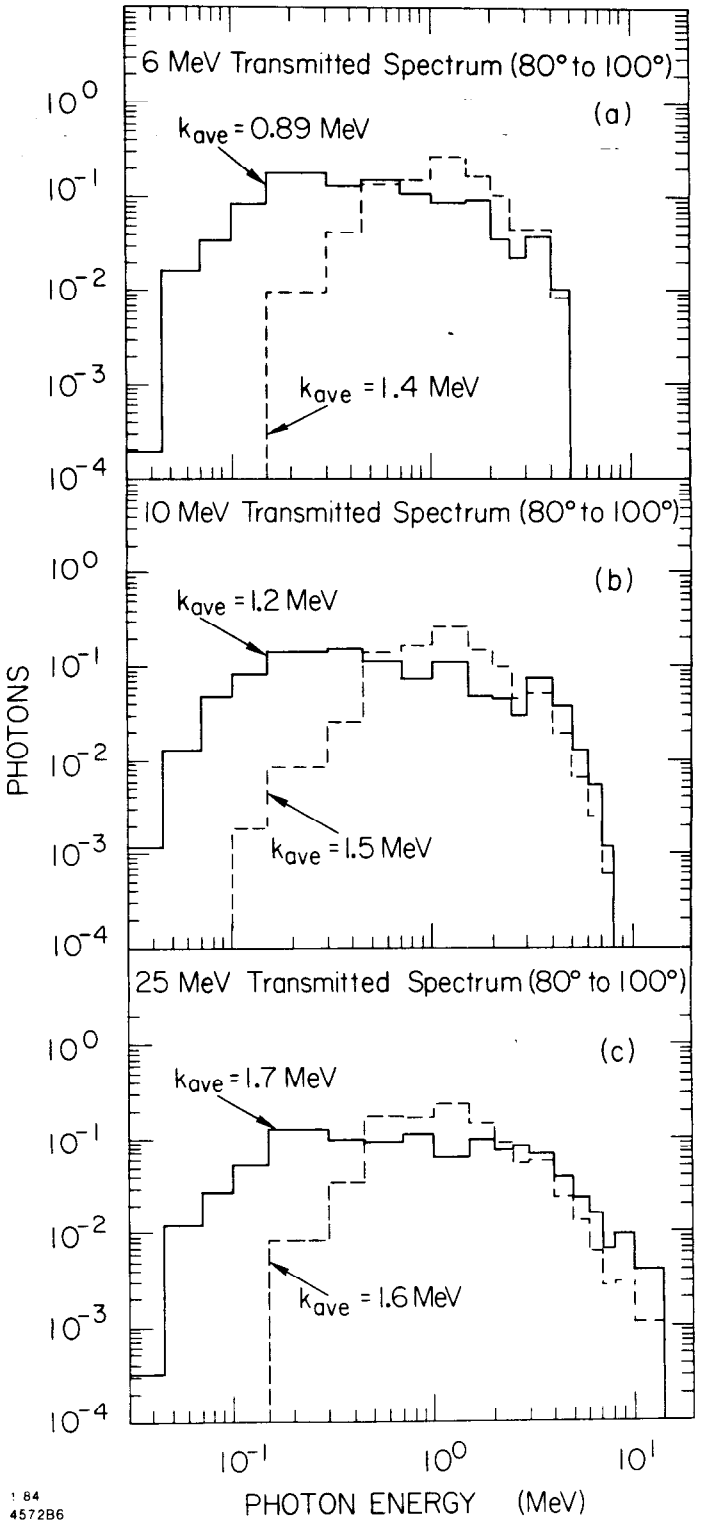
6 MeV Transmitted Spectrum (80° to 100°)
(a)
k_{ave} = 0.89 MeV
k_{ave} = 1.4 MeV
10 MeV Transmitted Spectrum (80° to 100°)
(b)
k_{ave} = 1.2 MeV
k_{ave} = 1.5 MeV
25 MeV Transmitted Spectrum (80° to 100°)
(c)
k_{ave} = 1.7 MeV
k_{ave} = 1.6 MeV
PHOTONS
10^{0}
10^{-1}
10^{-2}
10^{-3}
10^{-4}
10^{-1}
10^{0}
10^{1}
PHOTON ENERGY (MeV)
1 84
4572B6

Fig. 10